Quasi-Intersymbol Interference (QISI) Free Pulse Shaping

Rodolfo Norio Toma and Felix Antreich

***Abstract*— This work presents a methodology to achieve pulses with reduced intersymbol interference (ISI) and with improved data transmission performance. The designed pulses are obtained through the use of the prolate spheroidal wave functions (PSWF). An optimization problem is formulated to achieve maximum time-concentrated pulses and to ensure that they are ISI-free for a limited number of symbol durations, achieving what is called quasi-intersymbol interference (QISI) free. The resulting pulse designs are compared to relevant candidate Nyquist pulse designs from the literature and achieve comparable or enhanced performance for low to high timing errors.**

***Keywords*— Intersymbol interference (ISI), Nyquist pulses, pulse design.**

I. Introduction

The rapid growth of digital communications over the past decades imposes not only efficient use of bandwidth being a limited resource, but also higher data rates with less and less transmit power [1].

Significant research has been devoted to the development of intersymbol interference (ISI) free pulses, that guarantee distortionless transmissions, and additionally the development of pulse shaping filters with low sensitivity to timing errors [2]. In practical receivers the presence of timing jitter (synchronization errors) causes the actual sampling points to deviate from the optimal positions leading to timing errors [3]. Another source of timing errors in the receiver is multipath propagation [4].

Several contributions were made in pursue of the development of Nyquist pulses, since the contribution of Nyquist itself, from the the calculations used for error probabilities [5] to the design of pulses with enhanced performance, e.g., the "better than" raised cosine (BTRC) [6], the flipped-hyperbolic secant (fsech) and the flipped-inverse hyperbolic secant (farcsech) [7], the acos, acos[acos], acos[asech], acos[log], asech, asech[acos], asech[asech], asech[log], acos[exp], and asech[exp] pulses [2] [3], and the parametric linear combination pulses (PLCP) [8].

Taking another step forward in the development of strictly bandlimited pulses, this work develops a methodology to design pulses that follow the Nyquist ISI criterion and to maximize their time concentration. The proposed design methodology achieves quasi-ISI (QISI) free pulse designs by solving a quadratically constraint quadratic program (QCQP) problem [14] using the prolate spheroidal wave functions (PSWF) [9], [10] as basis functions to establish a parametric problem. The QCQP problem is maximizing time concentration of the pulse design and enforcing a specified number of zeros at multiple symbol duration T of the convolution of the transmit and the signal-matched receiver filter. This method can be considered as a framework for systematic pulse design with specific properties and performance for different applications and different degrees of timing errors. Such a systematic design methodology has not been presented so far in the literature for the design of ISI-free and especially QISI-free pulses.

Rodolfo Norio Toma, Brazilian Air Force, Aerospace Operations Command (COMAE), Brasilia-DF, e-mail: noriornt@fab.mil.br; Felix Antreich, Department of Telecommunications, Aeronautics Institute of Technology (ITA), São José dos Campos-SP, e-mail: fean@ita.br. This work was partially supported by the Brazilian National Council for Scientific and Technological Development (CNPq) under Grant 309248/2018-3 PQ-2 and 312394/2021-7 PQ-2.

II. System Model

We consider a basic transmission system with matched filtering, with a single transmitter and one receiver with a channel $h(t)$ as shown in the system block diagram in Figure 1. The baseband equivalent of a digital modulated signal can

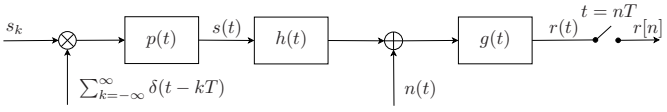

Fig. 1. System block diagram.

be given as

$$s(t) = \sum_{k=-\infty}^{\infty} s_k \, p(t - kT) \in \mathbb{C} \tag{1}$$

where s_k represents the discrete information sequence of symbols, $p(t)$ is the strictly bandlimited pulse shape with frequency response $P(f)$ with $P(f) = 0$ for $|f| > B$ and T is the symbol duration. We also assume that the channel has a response that is bandlimited to $[-B, B]$ with ideal frequency response characteristics, i.e., $H(f) = 1$. The baseband signal $s(t)$ passes through the channel $h(t)$ and is superimposed by complex additive white Gaussian noise $n(t)$ drawn from $\mathcal{CN}(0, \sigma_n^2)$. Then the received signal is fed through the receive filter $g(t)$ and we get the filtered output signal

$$r(t) = s(t) * g(t) + n(t) * g(t) = \sum_{k=-\infty}^{\infty} s_k \varphi(t - kT) + \tilde{n}(t) \tag{2}$$

where $\tilde{n}(t)$ denotes the noise at the output of the receive filter. Finally, after sampling in time intervals T we obtain the received symbols $r[n]$ with

$$r[n] = \sum_{k=-\infty}^{\infty} s_k \varphi[n - k] + \tilde{n}[n] \tag{3}$$

and $n = 0, \pm1, \pm2, \ldots$. To achieve maximum possible signal-to-noise-ratio (SNR) for the symbols s_k we have to choose the receive filter as the conjugate time-reversed as $g(t) = p^*(-t)$ and hence $\varphi(t) = p(t) * p^*(-t)$. We can reformulate (3) and we get

$$r[n] = s_n\varphi[0] + \underbrace{\sum_{\substack{k=-\infty \\ n\neq k}}^{\infty} s_k\varphi[n-k]}_{=\text{ISI}} + \tilde{n}[n]. \tag{4}$$

In order to achieve reception of the desired symbols without ISI the condition, which is called Nyquist ISI criterion, for $\varphi(t)$ can be given as

$$\varphi(nT) = \varphi[n] = \begin{cases} 1 & n = 0 \\ 0 & n \neq 0 \end{cases} \tag{5}$$

where we assume $\varphi[0] = 1$ without loss of generality.

III. Pulse Design Methodology

In this section we will introduce a pulse design method based on an optimization problem tailored to limit ISI.

A. Time Concentration

In order to facilitate implementation of the transmit and receive filters time concentration of $p(t)$ is an important property. Thus, the needed time support for the filters can be limited and a fast decay of $p(t)$ can be achieved. Time and frequency concentration of $p(t)$ can be given by

$$\bar{T} = \frac{\int_{-T/2}^{T/2} |p(t)|^2 dt}{\int_{-\infty}^{\infty} |p(t)|^2 dt} \quad \text{and} \quad \bar{B} = \frac{\int_{-B}^{B} |P(f)|^2 df}{\int_{-\infty}^{\infty} |P(f)|^2 df} \tag{6}$$

assuming

$$\int_{-\infty}^{\infty} |P(f)|^2 df = \int_{-\infty}^{\infty} |p(t)|^2 dt = 1. \tag{7}$$

In our case $\bar{B} = 1$ as we consider that $p(t)$ is strictly bandlimited to $[-B, B]$. Thus, due to the generalization of the uncertainty principle of the Fourier transform [11, p. 67] [12], [9] we get

$$\int_{-T/2}^{T/2} |p(t)|^2 dt = \bar{T} < 1. \tag{8}$$

It has been shown by Slepian, Landau, and Pollak in [12], [9] and by Papoulis in [11, p. 68] that for any time-bandwidth product $\varrho = TB$, $\bar{T} \leq \chi_0(\varrho)$ for $\bar{B} = 1$, where $\chi_0(\varrho)$ is the eigenvalue of the function $\psi_0(\varrho, t)$ which has the largest eigenvalue of a set of functions called the prolate spheroidal wave functions (PSWF) [10], [13]. Thus, for any ϱ the maximum time concentration in $[-T/2, T/2]$ for $\bar{B} = 1$ can be achieved when $p(t) = \psi_0(\varrho, t)$. This denotes the analytical solution for maximum time concentration of a strictly bandlimited pulse $p(t)$.

B. The Prolate Speroidal Wave Functions (PSWF)

The PSWF are particularly well suited to form a set of basis functions [12] to approximate bandlimited pulse shapes $p(t)$. They have the very interesting property of being orthogonal over two different intervals in the time domain.

For any $B > 0$ and $T > 0$ the PSWF form an infinite set of real functions $\psi_0(\varrho, t), \psi_1(\varrho, t), \psi_2(\varrho, t), \ldots$ with associated real positive eigenvalues $\chi_0(\varrho) > \chi_1(\varrho) > \chi_2(\varrho), \ldots$. The ψ_m and χ_m are functions of the normalized time-bandwidth product $\varrho = TB$. The $\psi_m(\varrho, t)$ are bandlimited to $[-B, B]$ and form a complete and orthonormal set of functions [12]

$$\int_{-\infty}^{\infty} \psi_m(\varrho, t)\, \psi_n(\varrho, t)\, dt = \begin{cases} 1, & m = n \\ 0, & m \neq n \end{cases}. \tag{9}$$

They also form a complete and orthogonal set in the interval $[-T/2, T/2]$ [12]

$$\int_{-T/2}^{T/2} \psi_m(\varrho, t)\, \psi_n(\varrho, t)\, dt = \begin{cases} \chi_m(\varrho), & m = n \\ 0, & m \neq n \end{cases}. \tag{10}$$

The PSWF are solutions of the integral equation [12]

$$\chi_m\, \psi_m(\varrho, t) = \int_{-T/2}^{T/2} \frac{\sin(2\pi B(t-s))}{\pi(t-s)}\, \psi_m(\varrho, s)\, ds. \tag{11}$$

The Fourier transform $\Psi_m(\varrho, f)$ of $\psi_m(\varrho, t)$ can be expressed in terms of $\psi_m(\varrho, t)$. Following [12], [11] we get

$$\Psi_m(\varrho, f) = \begin{cases} (-j)^m \sqrt{\frac{T}{\lambda_m 2B}}\, \psi_m(\varrho, f\, \frac{T/2}{B}) & \text{for } |f| \leq B \\ 0 & \text{else} \end{cases}. \tag{12}$$

Applying Parseval's theorem to (9) we get

$$\int_{-\infty}^{\infty} \Psi_m(\varrho, f)\, \Psi_n^*(\varrho, f)\, df = \begin{cases} 1, & m = n \\ 0, & m \neq n \end{cases}. \tag{13}$$

The $\psi_m(\varrho, t)$ are real, even for m even and odd for m odd. Their Fourier transform $\Psi_m(\varrho, f)$ is real and even for m even and imaginary and odd for m odd.

C. QISI-Free Pulse Design

In order to formulate a parametric optimization problem we use an expansion of the pulse shape $p(t)$ based on the PSWF dependent on the time-bandwidth product ϱ

$$p(t) = \sum_{m=0}^{M-1} x_m\, \psi_m(\varrho, t) \tag{14}$$

and

$$P(f) = \sum_{m=0}^{M-1} x_m\, \Psi_m(\varrho, f). \tag{15}$$

The expansion coefficients $x_m \in \mathbb{R}$ provide the weighting of the basis functions and enable parametrization of $p(t)$ and $P(f)$.

In this work we follow the strategy to design pulses that have a maximum time concentration which is not only beneficial for the implementation in a real system, but also reduces the effect of timing errors resulting from the tails of the pulses. Furthermore, we introduce up to K nulls at multiples of the

symbol period T of $\varphi(t)$ and we consider pulses of even or odd symmetry such that

$$\varphi(\pm kT) = 0, \quad \text{for} \quad k = 1, 2, \ldots, K. \tag{16}$$

Thus, to design pulses $p(t)$ that are maximum time-concentrated and that quasi fulfill the first Nyquist condition for up to K symbol durations T before and after the maximum of $\varphi(t)$ we can formulate the optimization problem

$$\max_{\mathbf{x}} \ \mathbf{x}^{\mathrm{T}}\mathbf{T}(\varrho)\mathbf{x} \tag{17}$$

subject to

$$||\mathbf{x}||_2^2 = \mathbf{x}^{\mathrm{T}}\mathbf{x} = 1 \tag{18}$$

$$\mathbf{x}^{\mathrm{T}}\mathbf{\Phi}_1(\varrho)\mathbf{x} = 0 \tag{19}$$

$$\vdots \quad \vdots$$

$$\mathbf{x}^{\mathrm{T}}\mathbf{\Phi}_K(\varrho)\mathbf{x} = 0 \tag{20}$$

where in order to maximize time concentration we can write

$$\int_{-T/2}^{T/2} \left(\sum_{m=0}^{M-1} x_m \, \psi_m(\varrho, t) \right) \left(\sum_{m=0}^{M-1} x_m \, \psi_m(\varrho, t) \right)^* dt$$
$$= \sum_{m=0}^{M-1} x_m^2 \chi_m(\varrho) = \mathbf{x}^{\mathrm{T}}\mathbf{T}(\varrho)\mathbf{x} \tag{21}$$

with

$$\mathbf{x} = [x_0, x_1, \ldots, x_{M-1}]^{\mathrm{T}} \in \mathbb{R}^{M\times 1} \tag{22}$$

$$\mathbf{T}(\varrho) = \mathrm{diag}\{[\chi_1(\varrho), \chi_2(\varrho), \ldots, \chi_{M-1}(\varrho)]^{\mathrm{T}}\} \in \mathbb{R}^{M\times M}. \tag{23}$$

The first constraint of the optimization problem introduces normalization of the power of $p(t)$ with

$$\int_{-\infty}^{\infty} \left(\sum_{m=0}^{M-1} x_m \, \Psi_m(\varrho, f) \right) \left(\sum_{m=0}^{M-1} x_m \, \Psi_m(\varrho, f) \right)^* df$$
$$= \sum_{m=0}^{M-1} x_m^2 \int_{-\infty}^{\infty} \Psi_m(\varrho, f)\Psi_m^*(\varrho, f) df = \mathbf{x}^{\mathrm{T}}\mathbf{x}. \tag{24}$$

The QISI-free constraints can be given by

$$\varphi(kT) = \int_{-\infty}^{\infty} P(f)P^*(f)e^{-\mathrm{j}2\pi fkT} df$$
$$= \sum_{m=0}^{M-1}\sum_{p=0}^{P-1} x_m x_p \int_{-\infty}^{\infty} \Psi_m(\varrho, f)\Psi_p^*(\varrho, f)e^{-\mathrm{j}2\pi fkT} df$$
$$= \mathbf{x}^{\mathrm{T}}\mathbf{\Phi}_k(\varrho)\mathbf{x} \tag{25}$$

where

$$\mathbf{\Phi}_k(\varrho) = \begin{bmatrix} \phi_{0\,0}(\varrho, k) & \cdots & \phi_{0\,P-1}(\varrho, k) \\ \vdots & \ddots & \vdots \\ \phi_{M-1\,0}(\varrho, k) & \cdots & \phi_{M-1\,P-1}(\varrho, k) \end{bmatrix}, \tag{26}$$

with

$$\phi_{m,p}(\varrho, k) = \int_{-\infty}^{\infty} \Psi_m(\varrho, f)\Psi_p^*(\varrho, f)e^{-\mathrm{j}2\pi fkT} df \tag{27}$$

and $k = 1, 2, \ldots, K$. The optimization problem described in (17), (18), (19), and (20) is a non-concave QCQP problem, as $\mathbf{T}(\varrho) \succeq 0$ and $\mathbf{\Phi}_k(\varrho)$ are indefinite [14]. We use the general *fmincon* function applying the interior-point algorithm of the Optimization Toolbox of MATLAB [15] to solve the QCQP problem initializing with $\mathbf{x} = [1, 0, \ldots, 0]^{\mathrm{T}}$.

IV. Performance Evaluation and Results

In this section we will discuss the performance and characteristics of the achieved pulse designs compared to pulse designs found in the literature.

A. Selected Pulse Characteristics

We selected pulse designs with $K = 11$ and $K = 16$ resulting from the QCQP. The pulses with $K = 11$ achieve a very low symbol error probability in the case of larger timing errors and the pulses with $K = 16$ achieve a similar symbol error probability compared to pulse designs found in the literature for lower timing errors when the sampling results closer to the optimum sampling point.

In Figures 2, 3, 4, and 5, $\varphi(t)$ is shown for the pulse designs with $K = 11$ and $K = 16$ compared to the classically used root-raised-cosine or square-root-raised-cosine (RRC) pulse [4] in the time and frequency domain for $\varrho = 0.675$, respectively. $\varphi(t)$ for the RRC is called raised cosine (RC) pulse [4].

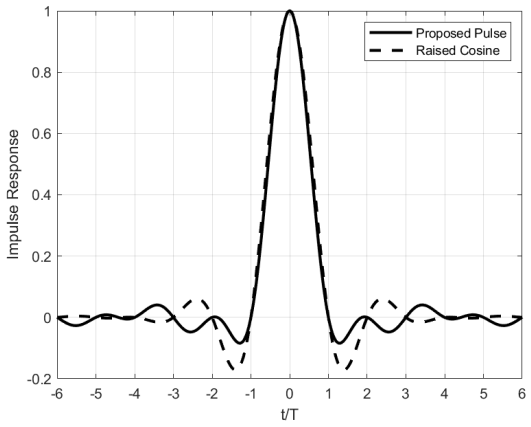

Fig. 2. Time domain of the RC pulse and the pulse design for $\varrho = 0.675$ and $K = 11$.

B. Eye Diagram

In this section we analyse the eye diagrams for the RC pulse and $\varphi(t)$ of the proposed pulse designs obtained by sampling two consecutive pulse periods of 2^9 consecutive pulses. Figure 6 shows the RC pulse's eye diagram and Figures 7 and 8 depict the eye diagrams for the pulse designs with $K = 11$ and $K = 16$ for $\varrho = 0.675$, respectively.

We can see that the eye opening is slightly wider for the two proposed pulse designs compared to the RC pulse which together with lower zero-crossing distortion indicates that the proposed pulse designs are less sensitive to timing errors [4]. However, we can also observe that at the optimum sampling point for the two proposed pulse designs the distortion is increased, which is the reason why we call our designs QISI-free pulses and which indicates that the proposed designs for zero timing error cause more ISI than the RC pulse.

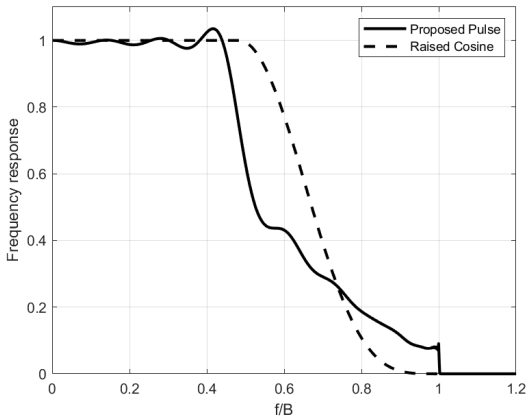

Fig. 3. Frequency domain of the RC pulse and the pulse design for $\varrho = 0.675$ and $K = 11$.

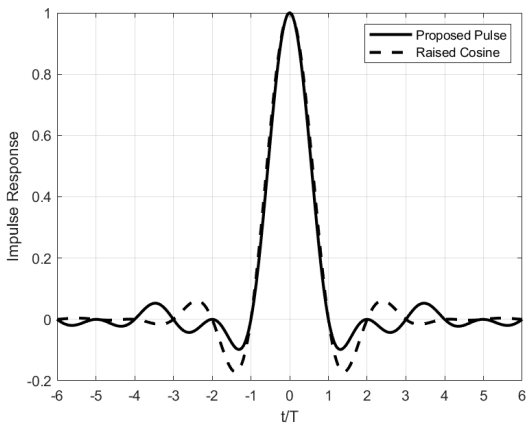

Fig. 4. Time domain of the RC pulse and time domain of the pulse design for $\varrho = 0.675$ and $K = 16$.

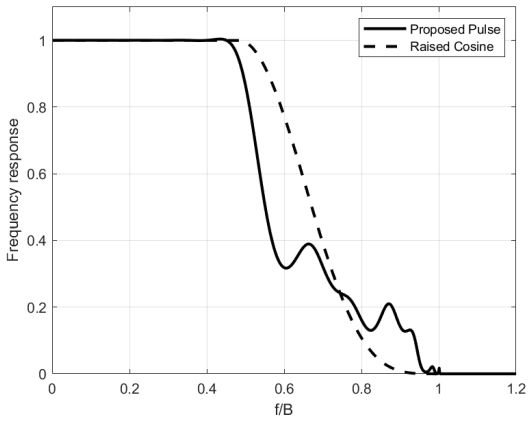

Fig. 5. Frequency domain of the RC and the pulse design for $\varrho = 0.675$ and $K = 16$.

C. Error Probability

In this section we compare the different pulse designs based on the resulting symbol error probability P_e. The P_e for a certain pulse shape can be derived following the method described in [5] with the number of coefficients considered in the truncated Fourier series $M = 99$, the period $T_f = 40$, 2^9 interfering symbols, and an SNR of 15 dB. The Tables I and II show P_e considering different timing errors t/T for the proposed pulse designs with $K = 11$ and $K = 16$, respectively.

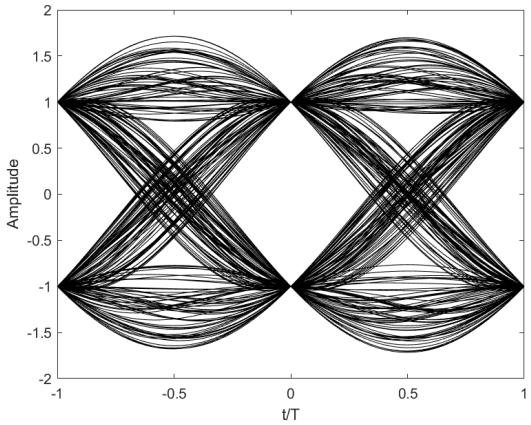

Fig. 6. Eye diagram of the RC pulse for $\varrho = 0.675$.

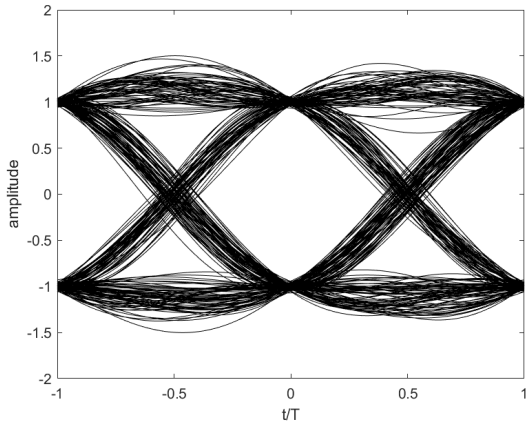

Fig. 7. Eye diagram of the pulse design for $\varrho = 0.675$ and $K = 11$.

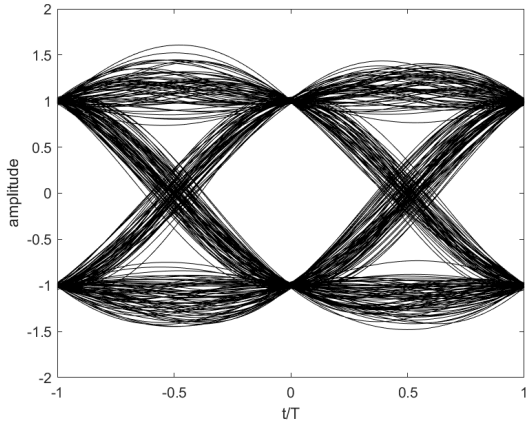

Fig. 8. Eye diagram of the pulse design for $\varrho = 0.675$ and $K = 16$.

TABLE I
ERROR PROBABILITY FOR $K = 11$ AND SNR $= 15$ dB

ϱ	$t/T = \pm 0.05$	$t/T = \pm 0.1$	$t/T = \pm 0.2$	$t/T = \pm 0.25$
0.625	6.7985e-8	9.9934e-7	1.9120e-4	0.0016
0.675	4.0431e-8	3.9518e-7	5.6022e-5	5.0937e-4
0.75	2.5105e-8	1.4241e-7	1.2900e-5	1.2691e-4
0.875	1.4655e-8	4.5241e-8	2.7108e-6	3.3311e-5
1	1.2667e-8	3.2560e-8	1.4673e-6	1.8016e-5

TABLE II
ERROR PROBABILITY FOR $K = 16$ AND SNR $= 15$ dB

ϱ	$t/T = \pm 0.05$	$t/T = \pm 0.1$	$t/T = \pm 0.2$	$t/T = \pm 0.25$
0.625	5.5215e-8	1.1667e-6	3.2115e-4	0.0026
0.675	3.9707e-8	5.0077e-7	9.3709e-5	8.4671e-4
0.75	2.3979e-8	2.0349e-7	3.0379e-5	3.0199e-4
0.875	1.4474e-8	4.9103e-8	3.4403e-6	4.2803e-5
1	1.2667e-8	3.2570e-8	1.4685e-6	1.8030e-5

Comparing P_e in Tables I and II we can observe that the designed pulses for $K = 11$ are more suitable for systems with larger timing errors and the designed pulses for $K = 16$ are more suitable for systems with smaller timing errors.

Tables III, IV, and V show P_e for the proposed pulse designs for $K = 11$ and $K = 16$ (called PPK11 and PPK16), the RC, the BTRC [6], the fsech and farcsech [7], the acos, acos[acos], acos[asech], acos[log], asech, asech[acos], asech[asech], asech[log], acos[exp], asech[exp] pulses [2], [3], and the PLCP [8].

TABLE III
ERROR PROBABILITY FOR $\varrho = 0.625$ AND SNR $= 15$ dB

Pulse	$t/T = \pm 0.05$	$t/T = \pm 0.1$	$t/T = \pm 0.2$	$t/T = \pm 0.3$
PPK11	6.7985e-8	9.9934e-7	1.9120e-4	0.0085
PPK16	5.5215e-8	1.1667e-6	3.2115e-4	0.0125
RC	8.2189e-8	2.8184e-6	9.7462e-4	0.0259
BTRC	5.8117e-8	1.2980e-6	3.5678e-4	0.0145
fsech	7.5579e-8	2.3337e-6	7.7201e-4	0.0230
farcsech	5.3996e-8	1.1011e-6	2.8405e-4	0.0125

TABLE IV
ERROR PROBABILITY FOR $\varrho = 0.675$ AND SNR $= 15$ dB

Pulse	$t/T = \pm 0.05$	$t/T = \pm 0.1$	$t/T = \pm 0.2$	$t/T = \pm 0.3$
PPK11	4.0431e-8	3.9518e-7	5.6022e-5	0.0034
PPK16	3.9707e-8	5.0077e-7	9.3709e-5	0.0052
RC	5.9997e-8	1.3896e-6	3.9084e-4	0.0155
BTRC	3.9253e-8	5.4021e-7	1.0129e-4	0.0059
fsech	5.4002e-8	1.0944e-6	2.8000e-4	0.0125
farcsech	3.5970e-8	4.4580e-7	7.6203e-5	0.0047
PLCP	3.9271e-8	5.9872e-7	9.9346e-5	-
acos	3.3527e-8	3.9249e-7	6.5764e-5	4.1127e-3
acos-acos	3.2753e-8	3.7964e-7	6.4348e-5	4.0152e-3
acos-asech	3.3558e-8	3.9255e-7	6.5582e-5	4.1067e-3
acos-log	3.5470e-8	4.3365e-7	7.3486e-5	4.5509e-3
asech	3.5970e-8	4.4581e-7	7.6204e-5	4.6951e-3
asech-acos	3.2264e-8	3.7363e-7	6.4494e-5	4.0024e-3
asech-asech	3.2255e-8	3.7275e-7	6.4110e-5	3.9850e-3
asech-log	4.2145e-8	6.2866e-7	1.2567e-4	7.0123e-3
acos-exp	3.3806e-8	3.9786e-7	6.6617e-5	4.1638e-3
asech-exp	3.2591e-8	3.7775e-7	6.4445e-5	4.0128e-3

We can observe in Tables III, IV, and V that PPK16 achieves a comparable P_e for small timing errors with $t/T \leq \pm 0.05$ with respect to all other pulse designs. For timing errors $t/T \geq \pm 0.1$ PPK11 achieves comparable or lower P_e than all the other considered candidate pulses. Thus, as discussed above, PPK11 provides higher robustness for larger timing errors.

V. CONCLUSION

This work developed a methodology for designing QISI-free pulses solving a QCQP problem using the PSWF and aiming to achieve a better performance, especially in case of timing errors. The proposed designs, PPK11 and PPK16, achieve comparable or better symbol error probability P_e compared to the main pulse designs found in the literature. It could be shown that for low timing errors the peak distortion effects are more dominant while for larger timing errors a fast decay of the pulse and thus a high time-concentration is beneficial.

TABLE V
ERROR PROBABILITY FOR $\varrho = 0.75$ AND SNR $= 15$ dB

Pulse	$t/T = \pm 0.05$	$t/T = \pm 0.1$	$t/T = \pm 0.2$	$t/T = \pm 0.3$
PPK11	2.5105e-8	1.4241e-7	1.2900e-5	0.0011
PPK16	2.3979e-8	2.0349e-7	3.0379e-5	0.0023
RC	3.9723e-8	5.4890e-7	1.0217e-4	0.0060
BTRC	2.4134e-8	1.8580e-7	2.0878e-5	0.0016
fsech	3.4949e-8	4.1186e-7	6.6009e-5	0.0042
farcsech	2.1875e-8	1.4916e-7	1.5344e-5	0.0012
PLCP	2.4356e-8	1.8659e-7	1.9743e-6	-
acos	2.0431e-8	1.3300e-7	1.4717e-5	1.2578e-3
acos-acos	2.0054e-8	1.3014e-7	1.5328e-5	1.3642e-3
acos-asech	2.0438e-8	1.3273e-7	1.4563e-5	1.2421e-3
acos-log	2.1559e-8	1.4514e-7	1.4987e-5	1.2082e-3
asech	2.1875e-8	1.4917e-7	1.5345e-5	1.2253e-3
asech-acos	1.9865e-8	1.2958e-7	1.6248e-5	1.4975e-3
asech-asech	1.9845e-8	1.2902e-7	1.6057e-5	1.4781e-3
asech-log	2.6157e-8	2.1763e-7	2.5364e-5	1.8850e-3
acos-exp	2.0583e-8	1.3446e-7	1.4657e-5	1.2385e-3
asech-exp	1.9992e-8	1.3005e-7	1.5658e-5	1.4094e-3

REFERENCES

[1] S. Assimonis, M. Matthaiou, G. Karagiannidis, "Two-parameter Nyquist pulses with better performance", *IEEE Communications Letters*, v.12, pp. 807–809, 2008, doi: 10.1109/LCOMM.2008.081117.

[2] S. Assimonis, M. Matthaiou, G. Karagiannidis, and J. Nossek, "Improved parametric families of intersymbol interference-free Nyquist pulses using inner and outer functions", *IET Signal Processing*, v.5, 157-163, Apr. 2011, doi: 10.1049/iet-spr.2009.0267.

[3] S. D. Assimonis, M. Matthaiou, G. K. Karagiannidis and J. A. Nossek, "Parametric Construction of Improved Nyquist Filters Based on Inner and Outer Functions," *2009 IEEE International Conference on Communications*, 2009, pp. 1-5, doi: 10.1109/ICC.2009.5199301.

[4] J. Proakis and M.Salehi, "Digital Communications", *McGraw-Hill*, 2008.

[5] N. Beaulieu, "The evaluation of error probabilities for intersymbol and cochannel interference", *IEEE Transactions On Communications*, v.39, pp. 1740-1749, Dec. 1991, doi: 10.1109/26.120161.

[6] N. C. Beaulieu, C. C. Tan, and M. Damen, "A "better than" Nyquist pulse", *IEEE Communications Letters*. v.5, pp. 367-368, Sept. 2001, doi: 10.1109/4234.951379.

[7] A. Assalini, and A. Tonello, "Improved Nyquist pulses", *IEEE Communications Letters*. v.8, 87-89, 2004, doi: 10.1109/LCOMM.2004.823414.

[8] C. A. Azurdia-Meza and C. Estevez, "Nyquist parametric linear combination pulses with better performance," *2014 9th International Symposium on Communication Systems, Networks & Digital Sign (CSNDSP)*, pp. 977-981, 2014, doi: 10.1109/CSNDSP.2014.6923971.

[9] H. Landau and H. Pollak, "Prolate Spheroidal Wave Functions, Fourier Analysis and Uncertainty - II", *Bell Systems Technology Journal*. v.40, pp. 65-84, Jan. 1961, doi: 10.1002/j.1538-7305.1961.tb03977.x.

[10] C. Flammer, *Spheroidal Wave Functions*, Stanford, CA: Stanford Univ. Press, 1957.

[11] A. Papoulis, "The Fourier Integral and its Applications", *McGraw-Hill Book Company Inc.*, 1962.

[12] D. Slepian, and H. O. Pollak, "Prolate Spheroidal Wave Functions, Fourier Analysis and Uncertainty - I", in *Bell Systems Technology Journal*, v.40, pp. 43-63, Jan. 1961, doi: 10.1002/j.1538-7305.1961.tb03976.x.

[13] S. Zhang, & J. Jin, "Computation of Special Functions", *John Willey & Sons, Inc.*,1996.

[14] S. Boyd and L. Vandenberghe, *Convex Optimization*, Cambridge: Cambridge University Press, 2004.

[15] "MathWorks Optimization Toolbox™ User's Guide", *The MathWorks, Inc.*,2022.